Applied Energy Symposium 2020: Low carbon cities and urban energy systems
October 10-17, 2020
Paper ID: xxxx

Design of Integrated Liquid Cooling System for An All SiC 650 V, 116 A Silicon Carbide MOSFET Power Module

Feng Han, Hong Guo, Xiao-feng Ding*

School of Automation Science and Electrical Engineering, Beihang University, Beijing, 100191, China

ABSTRACT

In this paper, the thermal performance of an all SiC 650 V, 116 A MOSFET power module has been studied by numerical simulation. Aiming at the heat dissipation problem of the SiC power devices in the inverter, three integrated liquid cooling heat sinks with different channel structures were designed. The results showed that compared with the other two cooling structures, the serpentine flow channel cooling structure can provide the best cooling effect. For the serpentine flow channel cooling structure, the heat source maximum temperature increases as the fin thickness increases, and the pressure drop decreases as the fin thickness increase when the coolant flow rate is constant. The improved heat sink has been numerical tested up to 110 A showing the device maximum temperature of 39.8°C, which can well meet the design requirements.

Keywords: liquid cooling, Silicon carbide, SiC MOSFET, power device, heat sink

NONMENCLATURE

Abbreviations	
SiC	silicon carbide
Symbols	
A	area (m^2)
h	convective heat transfer coefficient [W/(m2·K)]
t	temperature (°C)
λ	thermal conductivity [W/(m·K)]
Φ	heat (J)

1. INTRODUCTION

Smaller products with higher functional density are the eternal goal in the electronics industry. This requires the development of higher power density electronic devices with higher operating temperatures. However, the application of power electronics in military and automotive control electronics has reached the temperature limit of silicon electronics (about 150°C). Some alternative materials such as silicon carbide (SiC) wide band gap semiconductors are currently being studied by researchers [1-2]. Therefore, it is necessary to develop efficient cooling technologies that can handle these higher power densities [3].

The cooling of power devices is mainly divided into two categories: forced air cooling and integrated liquid cooling. Forced liquid cooling has a higher order of convective heat transfer coefficient when compared with forced air cooling. Many scholars have focused on various high heat flux liquid cooling technologies for power converter modules. Urciuoli et al. [4] built a 1200 V, 400 A SiC MOSFET module in a half bridge configuration with a thin integrated liquid-cooled heat sink. They proved that the high power converters using high temperature coolant can be successfully applied to the development of multi-chip all SiC switch modules. Boteler et al. [3] studied the thermal characteristics of an all SiC 1200 V, 400 A dual MOSFET power module with an integrated liquid cooling system. The results showed that when the input power is 158 W/cm^2, the device temperature rise is only 25°C. However, many studies focus on the influence of coolant temperature and flow rate changes [5] on the cooling effect, relatively little attention has been paid to changes in the fin size and channel layout inside the heat sink.

The primary objective of the current study is to investigate the influence of the three different channel layout structures on the cooling effect through numerical simulation. Taking the structure of the channel layout with the best cooling effect as the object of optimization, further study the influence of varying fin thickness and coolant flow rate on the cooling effect.

2. SIC POWER DEVICE AND LOSS ANALYSIS

2.1 SiC power device

SiC MOSFET is SCTH90N65G2V-7 produced by STPOWER company. The high operating junction temperature of the SiC MOSFET is 175°C. There are 12 SiC power devices on the power board, as shown by the blue rectangle in Fig. 1.

Selection and peer-review under responsibility of the scientific committee of CUE2020

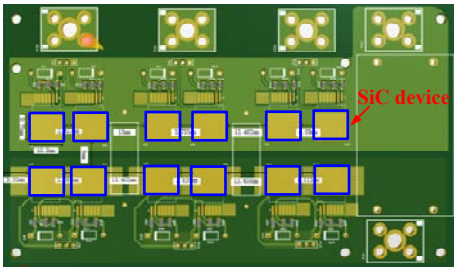

Fig. 1 Distribution of SiC devices on the power board

2.2 *Loss model of inverter*

The conduction loss of MOSFET can be expressed as,

$$P_{\mathrm{Con}} = I_{\mathrm{rms}}^2 R_{\mathrm{DS(on)}} \tag{1}$$

where P_{Con} indicates the conduction loss of MOSFET, I_{rms} is the effective value of phase current, $R_{\mathrm{DS(on)}}$ is the on-resistance of MOSFET. When the effective value of phase current $I_{\mathrm{rms}} = 110\mathrm{A}$ and the on-resistance of two SiC power devices in parallel $R_{\mathrm{DS(on)}} = 9 \times 10^{-3}\Omega$, the conduction loss can be calculated as,

$$P_{\mathrm{Con}} = (110)^2 \times 9 \times 10^{-3} = 108.9\mathrm{W} \tag{2}$$

The switching loss of MOSFET can be expressed as,

$$P_{\mathrm{SW\_T}} = f_s(E_{\mathrm{on}} + E_{\mathrm{off}})\frac{2\sqrt{2}}{\pi} \cdot \frac{I_{\mathrm{rms}}}{I_{\mathrm{ref}}} \cdot \frac{V_{\mathrm{DC}}}{V_{\mathrm{ref}}} \tag{3}$$

where $P_{\mathrm{SW\_T}}$ is the switching of MOSFET, f_s indicates the switching frequency, E_{on} and E_{off} respectively indicate the turn-on and turn-off energy of MOSFET in the reference load current I_{ref} and the reference dc bus voltage V_{ref}, V_{DC} indicates the dc bus voltage of the inverter. The values of E_{on}, E_{off}, I_{ref} and V_{ref} can be obtained from the datasheets. Under the design conditions of the dc bus voltage of the inverter $V_{\mathrm{DC}} = 270\mathrm{V}$, the switching loss can be calculated as,

$$P_{\mathrm{SW\_T}} = 2 \times 10 \times 10^3 \times \left(130 \times 10^{-6} + 210 \times 10^{-6}\right) \times 0.9 \times \frac{110}{116} \times \frac{270}{650} = 2.71\mathrm{W} \tag{4}$$

The total loss of inverter can be expressed as,

$$P_{\mathrm{universal\_bridge}} = 6 \times \left(P_{\mathrm{Con}} + P_{\mathrm{SW\_T}}\right) \tag{5}$$

Thus, the total loss of inverter can be calculated as,

$$P_{\mathrm{universal\_bridge}} = 669.66\mathrm{W} \tag{6}$$

2.3 *The principle and basic method of heat transfer*

First, the heat generated by the SiC device during operation is transferred to the heat sink through the contact surface, and this heat transfer method is heat conduction. Secondly, the heat transfer process in which the fluid flows through the inner surface of the heat sink to take away the heat is the convective heat transfer.

For any micro-element layer with a thickness of dx in the x direction, according to Fourier's law, the heat conduction heat passing through the plate per unit time is proportional to the local temperature change rate and the plate area A, that is:

$$\Phi = -\lambda A \frac{dt}{dx} \tag{7}$$

where Φ is heat, λ is thermal conductivity, the negative sign indicates the direction of heat transfer is opposite to the direction of temperature rise. The basic formula for convective heat transfer is the Newton's law of cooling:

$$\Phi = hA\Delta t \tag{8}$$

where Φ still indicates heat, h is the convective heat transfer coefficient, A is the effective contact area of heat convection, Δt is the temperature difference between the solid surface and the regional fluid.

3. NUMERICAL METHOD

3.1 *Validation of COMSOL model*

The simulations were performed using the commercial software COMSOL Multiphysics®. Boteler et al. [3] designed an integrated liquid cooling system for an all SiC 1.2 kV, 400 A dual MOSFET power module to reduce the thermal resistance. Fig. 2 shows the CAD drawing and material object of the heat sink.

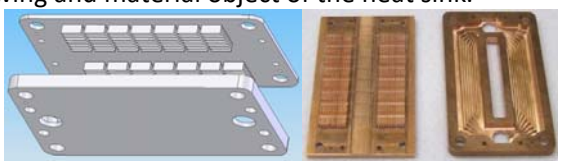

(a) CAD drawing (b) material object

Fig. 2 The heat sink model designed by Boteler et al.[4]

Under the condition that the physical filed used remains unchanged, the size of the heat sink was modified to the same form used by Boteler. The boundary conditions of the simulation were consistent with their experiment. A numerically simulation of the device temperature with various input powers was carried out under the same flow rate. Fig. 3 shows the rise in device temperature versus power compared with the experimental data of Boteler et al.

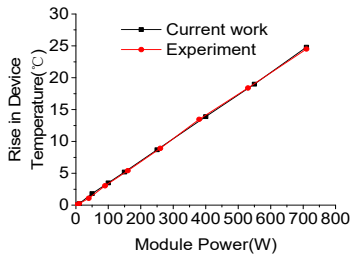

Fig. 3 Comparisons of the numerical results of the current work with the experimental results of Boteler et al. [4].

We can see that the results of the numerical simulations are in agreement with the previous

experimental data. The relative error between numerical simulation and experimental results is within 2%. This 2% prediction accuracy level is acceptable for the current work, therefore, the model can be applied to the predict the water cooling performance.

3.2 Computational model

According to the size of the PCB board, the corresponding geometrical models of the above three cooling schemes were established, as shown in Fig. 4.

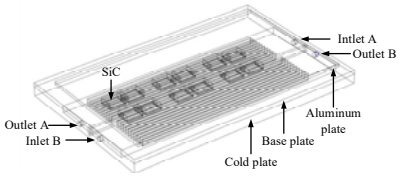

(a) The model of counter-flow channel cooling structure

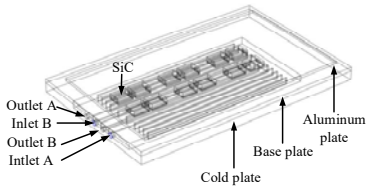

(b) The model of double U-shaped counter-flow channel cooling structure

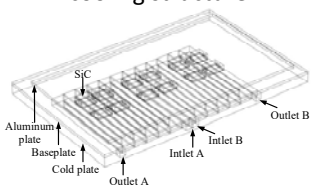

(c) The model of serpentine flow channel cooling structure

Fig. 4 Models of the three different cooling structures

For the counter-flow channel cooling structure [see Fig. 4(a)], a baffle is added in the middle of the cooling plate to divide the fluid domain into two symmetrical parts, so as to perform symmetrical counter-flow cooling of the power devices on the aluminum substrate. And the counter-flow method can improve the overall temperature uniformity of all SiC devices. For the double U-shaped counter-flow channel cooling structure [see Fig. 4(b)], the fluid domain is divided into two U-shaped channels inside and outside. Channels are added inside the U-shaped channels to increase the flow rate of the fluid in the channels. At the same time, the internal and external U-shaped channels are made countercurrent to improve temperature uniformity. The fluid flows. For the serpentine flow channel cooling structure [see Fig. 4(c)], the middle baffle divides the fluid domain into left and right parts. In order to improve the problem of heat stacking in the middle area, the fluid inlets were placed under the middle device.

Fig. 5 shows the channel layout in the water-cooling plate. The height of the fin H_{fin} is 5 mm and the width of the fin W_{fin} is 1 mm. The base plate thickness H_{base} of the water-cooling plate is 2 mm. The channel width W_{ch} of the counter-flow channel cooling structure (Case 1), the double U-shaped counter-flow channel cooling structure (Case 2) and the serpentine flow channel cooling structure (Case 3) are set to 2, 4 and 5 mm, respectively.

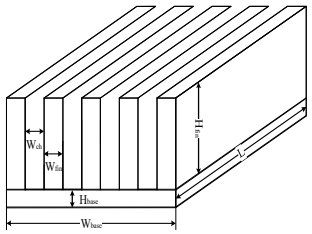

Fig. 5 Schematic diagram of channel layout

The above three cooling structural models were divided into grids respectively. The number and quality of grids are shown in Table 1. Considering the complexity of fluid flow and heat transfer, the fluid domain, fluid inlet and outlet positions were respectively refined.

Table 1: The number and quality of grids

Item	Case 1	Case 2	Case 3
Mesh number	597654	497104	518691
Mesh quality	0.7077	0.7239	0.7229

4. RESULTS AND DISCUSSION

All the simulations have been performed with the physical field of heat transfer in solids and fluids, and the multiphysics interface used nonisothermal flow. The natural convection of the air around the motor drive was ignored. When the motor drive system was running stably, the heat source loss obtained by theoretical calculation was 669.66 W. Water was used as the cooling medium. The material water cooling plate is aluminum alloy. And the inlet flow rate and temperature of the water were set to 2 L/min and 20°C, respectively.

4.1 Effect of cooling structure

The thermal simulation results of the three different cooling structures are shown in Figs. 6-8, respectively. As can be seen from Figs. 6-8, the highest temperatures of SiC devices obtained by the three cooling structures are 52.6°C, 54.8°C and 40.8°C, respectively.

For the counter-flow channel cooling structure (see Fig.6), the temperature distribution is not uniform. The four devices in the middle position have higher temperatures, while the lower left and upper right areas have lower temperatures. This is because the SiC devices on the lower left and upper right areas are close to the inlets of the A and B flow channels, respectively. And the fluid at the inlet of the channel has a lower temperature and a stronger cooling capacity. If the baffle between the

two flow channels is adiabatic, the temperature of the fluid will become higher and higher along the flow direction due to the heat of the fluid will gradually accumulate the fluid flows forward. However, the heat conduction phenomenon occurs in the baffle perpendicular to the fluid due to the temperature difference between the fluids on both sides of the baffle between the two flow channels in actual conditions. Compared with the baffle in the middle area, the baffle at the fluid inlet transfers more heat energy through heat conduction because of the larger temperature difference. In other words, due to the heat conduction phenomenon of the baffle, the temperature of the device areas at the farthest point downstream of the flow channel decreases and the temperature of the device areas at the fluid inlet increases. As a result, the four devices area have the highest level of temperature because of the counter-flow cooling arrangement.

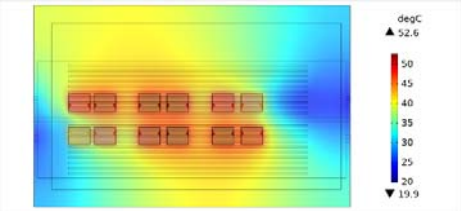

Fig. 6 Thermal simulation results of the counter-flow channel cooling structure

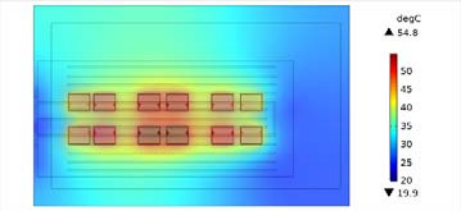

Fig. 7 Thermal simulation results of the double U-shaped counter-flow channel cooling structure

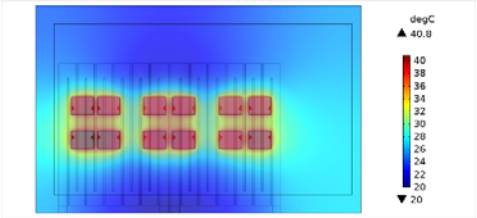

Fig. 8 Thermal simulation results of the serpentine flow channel cooling structure

For the double U-shaped counter-flow channel cooling structure (see Fig. 7), the temperature uniformity is slightly improved when compared with the counter-flow channel cooling structure. Moreover, the temperature distribution on the cooling area has a certain symmetry. Although the four devices in the middle position still have higher temperatures, the temperature of the device areas on the sides has decreased significantly. This may be because the inner U-shaped flow channel contains only 4 channels. When the flow rate is the same, the fluid velocity is large and the heat exchange capacity is relatively strong.

For the serpentine flow channel cooling structure (see Fig. 8), the temperature distribution is very uniform and the overall temperature of each device has little difference, which effectively avoids the problem of temperature accumulation of the four devices in the middle position. In addition, the temperature distribution on the cooling area is symmetrical, and the area of the high temperature region of the four devices in the middle position is smaller than that of the four devices on both sides. In terms of the maximum temperature and the uniformity of temperature distribution, this cooling structure can provide the beast cooling effect compared with the other two structures.

The pressure loss of the counter-flow channel cooling structure, the double U-shaped counter-flow channel cooling structure and the serpentine flow channel cooling structure is 1799 Pa, 2247 Pa and 11785.8 Pa, respectively. It can be seen that the serpentine flow channel cooling structure has the largest pressure loss. This is because the arrangement of the serpentine flow channel leads to a long flow channel significantly increases the length of the flow channel and the loss along the way.

Figs. 9-11 show the fluid velocity distribution of the three different cooling structures, respectively. For the counter-flow channel cooling structure (see Fig. 9), it can be seen that a part of the cooling fluid flows along the 6 channels facing the fluid inlet. The maximum flow velocity (1.92 m/s) appears at the inlet and outlet positions and the average value of the flow velocity in the above 6 channels is about 0.9 m/s. The average flow velocity of the entire cooling zone is 0.1786 m/s. At the same time, a small part of the fluid on both sides of the fluid has an obvious backflow phenomenon when the cooling fluid flows to the entrance of the channel. In addition, there are only 6 channels in total with good fluidity and the fluid in other areas hardly flows, which makes a large part of the cooling capacity of the fluid wasted. Therefore, the design of this cooling structure is unreasonable.

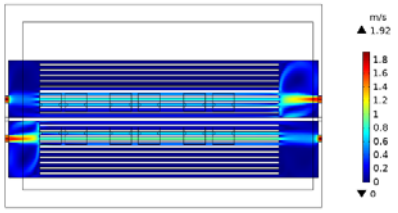

Fig. 9 The velocity profile results of the counter-flow channel cooling structure

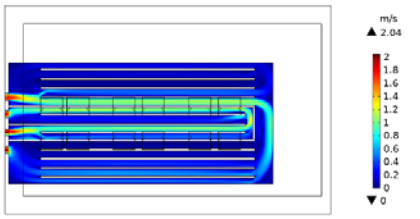

Fig. 10 The velocity profile results of the double U-shaped counter-flow cooling structure

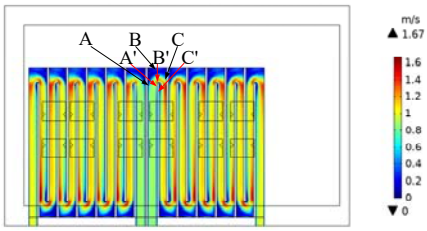

Fig. 11 The velocity profile results of the serpentine flow channel cooling structure

In order to further improve the cooling effect of the serpentine flow channel cooling structure, the influence of the thickness of the channel fin and the coolant flow rate on the cooling effect was studied on the basis of the existing model. The flow rate of cooling water varied from 1 L/min to 7 L/min and the channel fin thickness varied from 1 mm to 2 mm. The settings of other boundary conditions such as the heat source loss and the initial temperature of cooling water remains unchanged. The thickness of the channel fin was set to 1 mm, 1.2 mm, 1.5 mm, 1.8 mm and 2 mm, respectively. At the same time, the size of the cross-sectional area of the channel was kept unchanged. Fig. 12 shows the effect of different channel fin thickness on the heat source maximum temperature and pressure drop between the coolant inlet and outlet. Within the fin thickness range in this study, the heat source maximum temperature increases with the increase of the fin thickness.

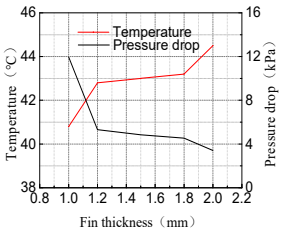

Fig. 12 The effect of fin thickness on the heat source maximum temperature and pressure drop

The temperature change rate is obviously different under different fin thickness conditions. When the fin thickness increases from 1 mm to 1.2 mm, the heat source maximum temperature increases by 2°C. When the fin thickness increases from 1.2 mm to 1.5 mm, the heat source maximum temperature increases by 0.2°C. When the fin thickness increases from 1.5 to 1.8 mm, the heat source maximum temperature also increases by 0.2°C. When the fin thickness increases from 1.8 to 2 mm, the heat source maximum temperature increases by 1.3°C. It can be found that the temperature change rate increases first and then decreases as the fin thickness increases. Different fin thicknesses cause corresponding changes in the total number of channels. When the fin thickness is set to 1 and 2 mm, there are 3 and less than 2 channels under heat source respectively. When the fin thickness is set to 1.2, 1.5 and 1.8 mm, there are 2 channels under each heat source. Therefore, this phenomenon shows the number of channels under the heat source has a greater impact on the cooling effect.

The pressure drop decreases as the fin thickness increases, which is the opposite trend to the changing law of temperature. This should be related to the number of channels and the total channel length. When the fin thickness is 1 mm, the number of channels is up to 24 and the total length of the channel is the longest. Due to the internal friction between the fluid layers and the friction between the fluid and the solid wall, the fluid produces greater flow resistance along a longer flow path. Moreover, the fluid flows through more elbows when compared with other fin thickness cases. When the fluid flows through the elbow, the impact between the fluid and the solid wall caused by the change of the fluid flow direction and velocity, the internal impact of the unequal velocity fluid and the vortex generated at the elbow will all produce flow resistance. The increase in the flow resistance of the coolant results in the largest pressure drop of 11.957 kPa. When the fin thickness is 1.2 mm, 1.5 mm, 1.8 mm and 2 mm, the corresponding pressure drops are 5.3158 kPa, 4.8479 kPa, 4.5384 kPa and 3.4108 kPa, respectively. Considering the best cooling effect, the fin thickness of 1 mm is a reasonable choice for the heat sink. However, the increase in pressure drop requires higher power of the pump that provides coolant fluid circulation. It is necessary to comprehensively consider that the coolant fluid can circulate stably under the actual pump operating conditions. Therefore, we believe that the fin thickness of 1.2 mm is more reasonable for the heat sink.

Fig. 13 shows the effect of different coolant flow on the heat source maximum temperature and pressure drop between the coolant inlet and outlet when the fin thickness is 1mm. The pressure drop gradually increases

as the coolant flow increases from 1 L/min to 7 L/min. This is because increasing the flow rate requires an increased driving force. And the pressure drop change rate tends to increase with an increase in the coolant flow. The heat source maximum temperature decreases continuously as the coolant flow increases. This is because increasing the flow rate can increase the exchange between the coolant and the cooling surface. And the change rate of the heat source maximum temperature also decreases with an increase in the coolant flow. Noted that the heat source maximum temperature decreases drastically as the coolant flow increases from 1 L/min to 3 L/min, and it decreases more gently as the coolant flow increases from 3 L/min to 7 L/min. This phenomenon shows that when the coolant flow is less than 3 L/min, the cooling capacity of the coolant is not enough to completely take away all the heat generated by the heat source. At this time, increasing the coolant flow will produce a better cooling effect. When the coolant flow exceeds 3 L/min, the degree of improving the cooling effect by increasing the coolant flow is not as obvious as before. In addition, considering that the pressure drop increases with the increase of the coolant inlet flow, we believe that it is reasonable to set the coolant flow to 3 L/min.

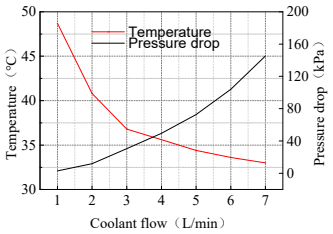

Fig. 13 the effect of coolant flow on the heat source maximum temperature and pressure drop

After changing the fin thickness of the heat sink from 1 mm to 1.2 mm, an improved cooling structure was obtained. The fluid flow rate was set to 3 L/min and the other boundary conditions were kept unchanged. Fig. 14 shows the thermal simulation results of the improved serpentine flow channel cooling structure.

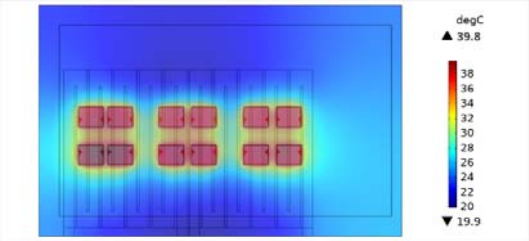

Fig. 14 Thermal simulation results of the improved serpentine flow channel cooling structure

The highest temperature of SiC devices obtained by the improved serpentine flow channel cooling structure is 39.8°C. The temperature distribution is very uniform and the temperature of all SiC devices is almost at the same level. Therefore, the improved heat sink has a good cooling effect and can meet the design requirements.

5. CONCLUSIONS

The thermal performance of an all SiC 650 V, 116 A MOSFET power module has been studied by numerical simulation in this paper. Three integrated liquid-cooled heat sinks with different channel structures were designed. The influence of the channel fin thickness and the coolant flow rate on the cooling effect was further studied on the basis of the existing model. The following conclusions can be made based on the numerical results:

(1) When the inlet temperature and flow rate of the coolant are the same, the serpentine flow channel cooling structure can provide a higher level of cooling effect than the other structures.

(2) For the serpentine flow channel cooling structure, the heat source maximum temperature increases as the fin thickness increases, which is the opposite trend to the changing law of pressure drop when the coolant flow rate is constant. The pressure drop increases as the coolant flow increases when the fin thickness is constant. The heat source maximum temperature decreases as the coolant flow increases.

(4) The highest temperature of SiC devices obtained by the improved heat sink is 39.8°C, which can well meet the design requirements.

REFERENCE

[1] Ding X, Du M, Zhou T, et al. Comprehensive comparison between silicon carbide MOSFETs and silicon IGBTs based traction systems for electric vehicles[J]. Applied Energy, 2016: S0306261916306560.

[2] Ding X, Du M, Duan C, et al. Analytical and Experimental Evaluation of SiC-Inverter Nonlinearities for Traction Drives Used in Electric Vehicles[J]. IEEE Transactions on Vehicular Technology, 2018, 67(1):146-159.

[3] Boteler L, Urciuoli D, Ovrebo G K, et al. Thermal performance of a dual 1.2 kV, 400 a silicon-carbide MOSFET power module[C]. semiconductor thermal measurement and management symposium, 2010: 170-175.

[4] Urciuoli D, Green R, Lelis A, et al. Performance of a dual, 1200 V, 400 A, silicon-carbide power MOSFET module[C]// Energy Conversion Congress & Exposition. IEEE, 2010.

[5] Jorg J, Taraborrelli S, Sarriegui G, et al. Direct Single Impinging Jet Cooling of a MOSFET Power Electronic Module[J]. IEEE Transactions on Power Electronics, 2017:1-1.